Functionalized metallic transition metal dichalcogenide (TaS_2) for nanocomposite membrane in direct methanol fuel cells

Hossein Beydaghi,[a] Leyla Najafi,[b] Sebastiano Bellani,[b] Ahmad Bagheri,[a] Beatriz Martín-García,[a] Parisa Salarizadeh,[c] Khadijeh Hooshyari,[d] Sara Naderizadeh,[e] Michele Serri,[a] Lea Pasquale,[f] Bing Wu,[g] Reinier Oropesa-Nuñez,[h] Zdeněk Sofer,[g] Vittorio Pellegrini,[ab] and Francesco Bonaccorso*[ab]

[a] *Graphene Labs, Istituto Italiano di Tecnologia, via Morego 30, 16163 Genova, Italy*

[b] *BeDimensional SpA, via Albisola 121, 16163 Genova, Italy*

[c] *High-Temperature Fuel Cell Research Department, Vali-e-Asr University of Rafsanjan, 7718897111 Rafsanjan, Iran*

[d] *Department of Applied Chemistry, Faculty of Chemistry, Urmia University, 5756151818 Urmia, Iran*

[e] *Smart Materials, Istituto Italiano di Tecnologia, via Morego 30, 16163 Genova, Italy*

[f] *Materials Characterization Facility, Istituto Italiano di Tecnologia, via Morego 30, 16163 Genova, Italy*

[g] *Department of Inorganic Chemistry, University of Chemistry and Technology Prague, Technická 5, 166 28 Prague 6, Czech Republic*

[h] *Department of Materials Science and Engineering, Uppsala University, Box 534, 75121 Uppsala, Sweden*

S.1 Experimental section

S.1.1. Materials

Powder of poly (ether ether ketone) (PEEK) (Mw: 28800 g mol^{-1}), sodium 3-mercapto-1-propane sulfonate salt (SMPS) (90%), dimethyl sulfoxide (DMSO) (≥ 99.9%), concentrated H_2SO_4 (95–98%) (sulfonation agent) and 1-methyl-2-pirrolidone (NMP) (solvents for PEEK, sulfonated PEEK (SPEEK) and tantalum disulfide functionalized with terminal sulfonate groups (S-TaS_2)) were purchased from Sigma Aldrich. Tantalum (99.9 %, <100 μm) and Sulphur powder (99.999 %, < 6mm) were supplied from Strem Chemicals. All chemicals were used as received without any further purification.

S.1.2. Sulfonation of PEEK

The powder of PEEK was sulfonated with different degree of sulfonation (DS) by direct sulfonation reaction with concentrated H_2SO_4, in agreement with the following procedure.[1] Firstly, PEEK powder was dried at 60 °C for 24 h and then a certain amount of dried PEEK powder was slowly dissolved in concentrated H_2SO_4 under stirring conditions at room temperature for 1 h. The ratio of PEEK and concentrated H_2SO_4 was maintained at 1/10 (w/v). After dissolving the polymer, the temperature of the resulting solution was raised to 60 °C and kept for different times (from 4 to 7 h) depending on the required DS (Table S1). The DS increased by increasing the duration of the sulfonation reaction. Subsequently, the solution is cooled down to room temperature. After that, the solutions were led to slowly precipitate into a large amount of ice cold water under mechanical agitation to recover the modified polymers. The obtained sulfonated polymers were washed with deionized water several times until achieving neutral pH, and dried in an oven at 70 °C for 24 h. The DS values of the prepared samples, listed in Table S1, were measured by means of titration method, in agreement with the following equation:

$$DS = \frac{10^{-3} \times 288.31 \times C_{NaOH}\ V_{NaOH}}{W - 0.081\ C_{NaOH}\ V_{NaOH}} \times 100$$

where, C_{NaOH} is the molar concentration of the NaOH solution, V_{NaOH} is the amount of the consumed NaOH solution, W is the weight of the tested SPEEK sample, 288.31 g mol^{-1} is the molecular weight of the PEEK unit, and 81 g mol^{-1} is the molecular weight of the SO_3H group.

Table S1. DS of the different SPEEK prepared using different reaction time

PEEK weight: concentrated H_2SO_4 volume (w/v)	Reaction temperature (°C)	Reaction time (h)	DS (%)
1/10	60	4.10	60.00
1/10	60	4.40	63.75
1/10	60	5.15	67.5
1/10	60	5.55	71.25
1/10	60	6.50	75.00

S.1.3. Synthesis of S-TaS_2 nanoflakes

Firstly, *6R*-TaS_2 crystals were synthesized from by direct reaction of their composing elements, Ta and S, following previous protocols reported for group-5 transition metal dichalcogenides.[2,3] The appropriate weight of Ta and S powders (Ta:S stoichiometry = 1:2) corresponding to 10 g of TaS_2 were placed into a quartz glass ampoule with a dimension of 20 mm x 120 mm. After reaching high vacuum (1×10^{-3} Pa) the ampoule was sealed by oxygen-hydrogen welding torch. Subsequently, the ampoule was heated to 450 °C for 12 h, and then to 600 °C for 48 h. Afterward, the obtained products were treated at 900 °C for 48 h, and then cooled down to room temperature

over 24 h. The heating rate was for all steps ±5 °C min^{-1}. The TaS_2 nanoflakes were produced by means of liquid-phase exfoliation (LPE) in anhydrous 2-propanol (IPA) of the as-produced crystals,[4,5] followed by sedimentation-based separation (SBS). Briefly, 500 mg of fragmentized crystals were added to 50 mL of anhydrous IPA and ultrasonicated in a sonicator (Branson® 5800 cleaner, Branson Ultrasonics) for 6 h. Then, the obtained dispersion was ultracentrifuged using a Beckman Coulter centrifuge (Optima™ XE-90 with a SW32Ti rotor) at 2700 *g* for 20 min at 15 °C to separate the exfoliated materials in the supernatant from the sediment consisting of unexfoliated bulk crystals. The exfoliated materials were collected by pipetting 80% of the supernatant, obtaining a dispersion of TaS_2 with a concentration of 0.86 g L^{-1}, as measured by gravimetric method.

The LPE-produced TaS_2 nanoflakes were functionalized using SMPS. Briefly, the functionalization was carried out by heating the as-produced TaS_2 nanoflakes dispersion at 70°C (temperature controlled with a thermocouple) for 5 h under vigorous magnetic stirring and adding 41 mg of SMPS (dispersed in 1 mL of DMSO per 1 mL of TaS_2 dispersion (10 mg mL^{-1} in IPA)). To remove the excess of SMPS, the material was first recovered by centrifugation (Sigma 3-16P centrifuge, rotor 19776) for 10 min at 2599 *g*. Then, the material was washed four times using IPA:DMSO (1.5:1 vol.) and once more only with IPA to remove the residues of DMSO, combining the redispersion of material through ultrasonication for 5 min with ultracentrifugation for 20 min at 106800 *g* (Sigma 3-16P centrifuge, rotor 19776). After the washing protocol, the S-TaS_2 nanoflakes were redispersed in NMP by ultrasonication for 20 min to obtain the final ink concentration of 18 mg mL^{-1}.

S.1.4. Membrane preparation

The SPEEK and SPEEK/S-TaS_2 membranes (hereafter named M_S and M_{runx}, respectively, in which x is the number of run provided to response surface methodology (RSM), were produced by the solution casting method.[1,6] According to Table 2, 13 runs of the solution casting method were used to achieve the optimum amount of nanoflakes and DS of SPEEK in the nanocomposite membrane through RSM. Firstly, the appropriate amount of SPEEK was dissolved in NMP (1/10 w/v) at 60 °C for 2 h. Afterward, according to the required weight percent of S-TaS_2 nanoflakes (0.5 - 2.5 wt%), appropriate amount of S-TaS_2 nanoflakes dispersed in NMP was added to the above solution and stirred for 4 h at the same temperature. Finally, the obtained solution was cast by the doctor blade on the glass sheet and dried at 80 ºC for 12 h, 120 ºC for 12 h, and 140 ºC for 4 h in vacuum. The pristine membrane was also produced using the same procedure, without adding the S-TaS_2 nanoflakes. The thickness of the dry prepared membranes is between 80–120 μm. The obtained nanocomposite membranes were treated in 1 M H_2SO_4 for 12 h before the experiments in order to activate and purify the membranes.[7]

S.1.5. Statistical and experimental design protocol

Mathematical designs represent reliable and time-saving solutions to minimize the number of experiments in presence of multiple system variables.[8,9] The experimental design was implemented by means of Design expert (version 8) software,[10] using central composite design (CCD)[11] in RSM analysis,[8] to investigate the impact of DS of SPEEK and the wt% of S-TaS_2 nanoflakes on the membrane properties, including water uptake (WU), membrane swelling (MS), proton conductivity (σ), methanol permeability (P) and selectivity (S). In this work, two key factors were selected as operating parameters that mainly influence the performance of the prepared membranes: the DS of SPEEK, ranging between 60 and 75 %, and the wt% of S-TaS_2 nanoflakes, ranging between 0.5 and 2.5 wt%. The experimental design was elaborated for five parameters of

DS of SPEEK, *i.e.*, 60.00, 63.75, 67.50, 71.25, and 75.00, and the wt% of the S-TaS_2 nanoflakes, *i.e.*, 0.5, 1.0, 1.5, 2.0, and 2.5, were varied to set the CCD. The trials were run in random order to avoid or minimize the effects of unexpected variable parameters in the obtained responses due to unrelated factors. As shown in Table 2, the effects of the DS of the polymer and the wt% of nanoflakes factors, influencing the responses, were investigated by 13 experiments, 5 of which were explored as a center point. To achieve the optimum DS of polymer and the wt% of the S-TaS_2 nanoflakes, the experimental design array was constructed to determine maximum WU and σ, minimum P and MS, together with the highest S.

S.1.6. Characterization of materials and membranes

The morphology of the as-produced nanoflakes was investigated by transmission electron microscopy (TEM) on a JEM 1011 (JEOL) TEM (thermionic W filament), operating at an acceleration voltage of 100 kV. The sample was prepared by drop-casting the LPE-produced nanoflake dispersions onto ultrathin C-on-holey C-coated Cu grids, subsequently washed with deionized water and dried in vacuum overnight. ImageJ software (NIH) and OriginPro 9.1 software (OriginLab) were used to perform the morphological and statistical analyses, respectively.

X-ray diffraction (XRD) analysis of the LPE TaS_2 nanoflakes before and after functionalization was carried out using the PANalytical Empyrean X-ray diffractometer with Cu Kα radiation. Raman measurements were acquired using a Renishaw microRaman Invia 1000 spectrometer, mounting a 50× objective with a 532 nm laser. The samples for XRD and Raman analysis were prepared by drop-casting the nanoflake dispersions onto substrates of Si/SiO_2, and then dried under vacuum overnight.

The X-ray photoelectron spectroscopy (XPS) analysis was performed on a Kratos Axis UltraDLD spectrometer at a vacuum < 10^{-8} mbar, using a monochromatic Al Kα source operating at 20 mA

and 15 kV and collecting photoelectrons from a 300 × 700 μm^2 sample area. Wide spectra were acquired at pass energy of 160 eV and energy step of 1 eV, while high-resolution spectra of Ta 4f, S 2p, O 1*s* and C 1 s peaks were acquired using a pass energy of 10 eV and an energy step of 0.1 eV. The samples were prepared by drop-casting the nanoflake dispersions on an Au-coated Si substrates while heating the substrates to 60°C. The samples were then transferred from air to the XPS chamber. The analysis of the XPS data was carried out with CasaXPS software (version 2.3.22PR1.0). The energy scale was calibrated by setting the C 1s adventitious peak at 284.8 eV.

Fourier-transform infrared (FTIR) spectra of the membranes were recorded using a single-reflection ATR accessory (MIRacle ATR, Pike Technologies) coupled to a FTIR spectrometer (Equinox 70 FT-IR, Bruker). All the spectra were measured in the wavelength range from 2000 to 600 cm^{-1}, with a resolution of 4 cm^{-1} and accumulating 128 scans. To ensure the reproducibility of the spectra, the measurements were performed on three different pieces of each sample.

Scanning electron microscopy (SEM) images of the nanoflakes and PEMs were acquired using JEOL JSM-6490LA SEM Analytical (low-vacuum) scanning electron microscope with a thermionic electron gun equipped with a W source. Prior to start, the membranes were coated with gold. Element mapping was accomplished with an energy dispersive X-ray spectroscopy.

Adhesion force/work measurements of the membranes were carried out using a Bruker Dimension Icon atomic force microscope (Bruker Dimension Icon, Billerica, MA, USA). Force volume measurements were acquired using V-shaped DNP silicon nitride cantilevers (Bruker, Billerica, MA, USA), with a nominal spring constant of 0.06 N m^{-1}, resonance frequency in air in the 40–70 kHz range and tip typical curvature radius of 20–60 nm. The actual spring constant of each cantilever was determined *in situ*, using the thermal noise method. The acquisition of a large set of force–distance curves (4096 curves) was performed in humid ambient air (relative humidity –

RH– ~75%) and in water with a maximum force load of 20 nN and a curve length of 800 nm per each sample. Adhesion force maps of 20 × 20 μm^2 were collected. The adhesion work data were analyzed with OriginPro 9.1 software.

Thermal degradation of membranes was evaluated using thermogravimetric analysis (TGA), TGA Q500 (TA Instruments, USA). The measurements were performed on 5 mg of the sample in Pt pans under inert (N_2) atmosphere. The membranes were heated from room temperature to 800 ºC with a heating rate of 10 ºC/min.

The tensile tests of the produced membranes were performed using the STM-50 testing machine (SANTAM, Iran), with a stretching rate of 2 mm min^{-1}.

The membranes WU was measured at different temperatures by soaking the membranes for 12 h in deionized water in controlled temperature conditions. The increase of membrane weight was measured with a balance. The WU value of the prepared membranes was calculated according to the equation:

$$WU\,(\%) = \frac{W_w - W_d}{W_d} \times 100$$ where,

W_w is the weight of the wet membrane, and W_d is the weight of the dry membranes.

The MS of the membranes were investigated by measuring the membrane dimension before (A_d) and after (A_w) soaking of the membrane for 12 h in deionized water, and calculated using the equation:

$$MS\,(\%) = \frac{A_w - A_d}{A_d} \times 100$$

The ion exchange capacity (IEC) of the produced membranes was investigated by the conventional titration method. A piece of membrane was completely immersed into a saturated NaCl solution

for 24 h, to exchange the H^+ with Na^+. The H^+ concentration in the resulting solution was titrated by a 0.01 mol L^{-1} NaOH solution, using phenolphthalein as an indicator. The IEC value of the produced membranes was calculated according to the equation:

$$IEC = \frac{V_{NaOH} \times C_{NaOH}}{W_{dry}}$$

where, V_{NaOH} and C_{NaOH} are the volume and concentration of the NaOH solution, respectively.

The oxidative stability of the membranes was investigated by immersing the membranes into a Fenton solution (3 wt% H_2O_2 + 2 ppm $FeSO_4$) at 80 °C. The Fenton solution was replaced with fresh solution every few hours due to the disadvantage of produced hydroxyl radicals to the membrane. The chemical stability of the membranes was measured over time until the breaking of membranes in pieces.

The σ measurements were carried out on different prepared membranes in a conductivity cell by AC impedance technique. The σ of the prepared membranes was calculated using a VMP3 multichannel potentiostat/galvanostat (Bio-Logic, France) controlled through Bio-Logic's own software. The frequency range was 100 kHz - 2 mHz and AC voltage was 50 mV. The samples were sandwiched between two Pt electrodes. Before the test, the samples were activated by immersion in deionized water for 12 h. The bulk resistance (R, Ω) was determined by the impedance plot according to the protocols described in [6]. The σ of the membranes was calculated according to the equation:

$$\sigma = \frac{L}{R.A}$$

in which, L is the thickness of the membrane, and A is the area of the membrane. The activation energy (E_a), *i.e.*, the minimum energy required for transferring a proton, for each membrane can be calculated using the Arrhenius equation $\sigma = A \exp(-E_a/RT)$, in which A is a pre-exponential factor, R is the universal gas constant (expressed in $Jmol^{-1}\ K^{-1}$), and T is the temperature (in K).

The P of the membranes was investigated by a home-made two-separate compartment diffusion cell. Briefly, the first compartment (A) was filled with 1.0 M methanol-deionized water solution and the second compartment (B) was filled with deionized water, which was separated by the different prepared membranes. Being the concentration of the methanol in the compartment A much higher than the one in the compartment B, methanol diffused through the membrane and the methanol concentration in the second compartment (B) was measured as a function of time using a density meter. The P of the membranes was calculated using the equation:

$$C_B(t) = \frac{AP}{LV_B} C_A(t - t_0)$$

in which, C_A and C_B are the methanol concentrations in the compartment A and B, respectively, A and L are the effective area and the thickness of the membrane, t is the permeability test time, and V_B is the volume of compartment B.

The S of the membranes is defined as the ratio of σ to P, and was measured using the equation:

$$S = \frac{\sigma}{P}$$

S.1.7. Direct methanol fuel cell (DMFC) performance

The DMFC performance was measured in membrane electrode assemblies (MEAs), using gas diffusion layers. The cathode catalyst ink was produced by mixing Pt/C (20 wt%), Nafion solution

(5 wt%), glycerol as the suspension agent, IPA, and deionized water. The mixture was ultrasonicated for 2 h to make a slurry which was then painted onto carbon cloths (E-Tek, HT 2500-W) and dried in oven. The anode catalyst ink was obtained by mixing Pt-Ru/C (40:40:20 wt%), Nafion solution (5 wt%), IPA, and deionized water. After obtaining a homogeneous slurry, the latter was deposited onto the carbon cloth. The catalyst loadings were 1 mg cm^{-2} and 2 mg cm^{-2} for cathode and anode, respectively. Finally, the prepared electrodes and membrane were hot-pressed at 140 °C for 3 min to form the MEA. The MEAs prepared with the different membranes were assembled with fixtures, current collectors, and methanol tank to obtain the DMFCs. Before DMFC test, the prepared MEAs were immersed in 2 M methanol solution for 3 h and activated under constant current of 15 mA cm^{-2} for 2 h. The performance of the DMFCs was evaluated at different temperatures on an Arbin FCT testing system (Arbin Instrument Inc. USA) by using 2 M aqueous methanol solution and O_2 with zero backpressure at the flow rate of 2 mL min^{-1} and 300 mL min^{-1} at anode and cathode, respectively. The long-term stability of the optimized membrane (M_{opt}) was evaluated by measuring the open circuit voltage (OCV) *versus* time (200 h) of the corresponding DMFC.

S2. FTIR spectroscopy analysis of the membranes

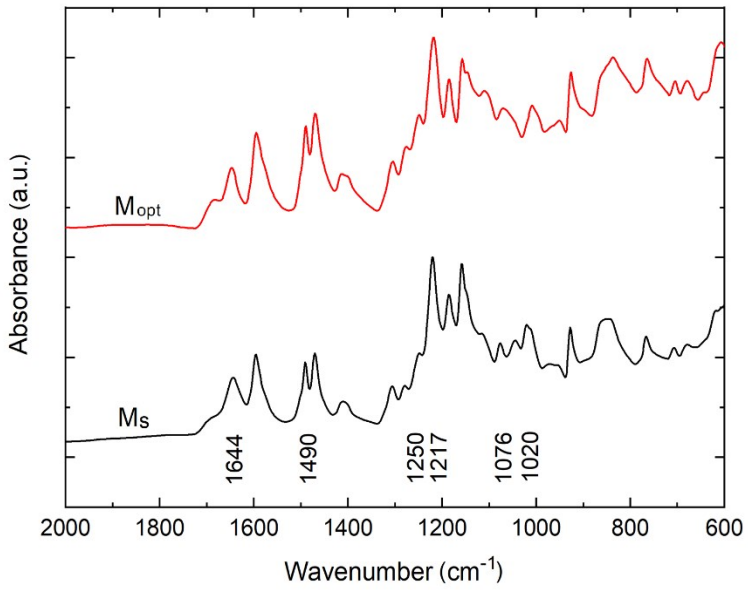

Fig. S1 FTIR spectra of the M_S, and M_{opt}.

Fig. S1 shows the FTIR spectrum of M_S and a representative S-TaS_2 nanocomposite membrane, *i.e.*, the optimized membrane (M_{opt}) (see optimization details in Experimental section and in the subsequent optimum condition section). The peaks around 1217 and 1490 cm^{-1} are due to the vibration of the C–O–C and C–C aromatic ring in the polymer.[12] The observed absorption peak around 1644 cm^{-1} is assigned to the existence of the carbonyl band of SPEEK.[13] Due to the introduction of sulfonated groups, sulfonated polymers were shown strong characteristic peaks at 1020, 1076, and 1250 cm^{-1}, which corresponded to asymmetric and symmetric stretching vibration of O=S=O and stretching vibration of S=O, respectively.[14] In the nanocomposite membrane, the difference in the shape and intensity of asymmetric and symmetric O=S=O bonds is due to the more available sulfonated groups and direct condensation reaction between sulfonic acid groups of S-TaS_2 nanoflakes and SPEEK.

S3. IEC of the membranes

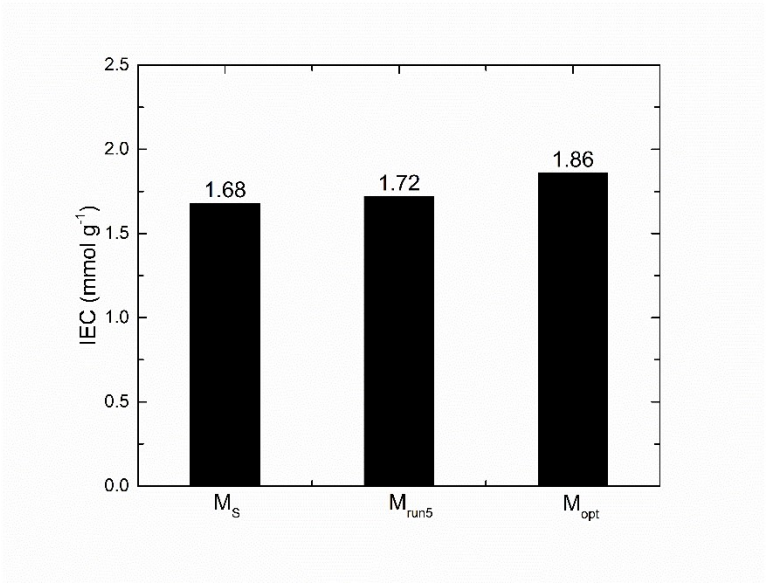

Fig. S2 IEC of the M_S, M_{run5} and M_{opt}.

The IEC is a useful parameter to determine the density of proton exchangeable groups in the membrane structure. The IEC of the M_S, M_{run5} and M_{opt} membranes was measured and results are shown in Fig. S2. The M_S, M_{run5}, and M_{opt} membranes show an IEC of 1.68, 1.72, and 1.86 mmol g^{-1}, respectively. The M_{run5} membrane, despite it shows DS of the polymer (67.5 %) lower than the one of M_S membrane (70.2 %), exhibits higher IEC (1.72 mmol g^{-1}) due to the presence of supplementary ion exchangeable groups (sulfonated groups) in the S-TaS_2 structure. In addition, the results of Fig. S2 show that the IEC value increased from 1.72 mmol g^{-1} in the M_{run5} to 1.86 mmol g^{-1} in the M_{opt}, which is due to the higher DS of SPEEK in the M_{opt} (70.2 %) compared to the M_{run5} (67.5 %) membrane and the presence of supplementary ion exchangeable groups (−SO_3H groups) in the S-TaS_2 nanoflakes. The increase of IEC corresponds to a decrease of the distance between ion exchangeable groups, resulting in fast proton transfer in the membrane.

S.4 E_a of membranes

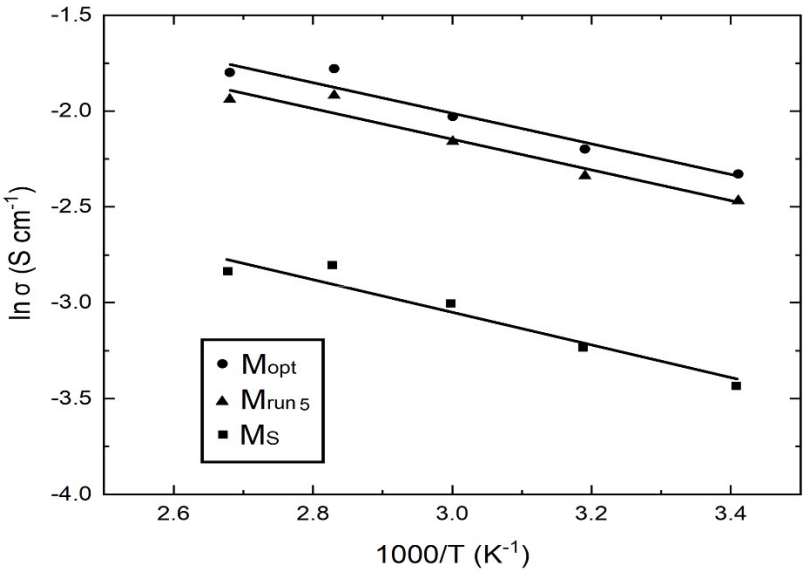

Fig. S3 Arrhenius plot of the σ of the M_S, M_{run5} and M_{opt}.

The σ of different prepared membranes at different temperatures (Arrhenius curves) are shown in Fig. S3. The nanocomposite membranes exhibit higher σ (84.11 and 96.24 mS cm^{-1} for M_{run5} and M_{opt}, respectively) than the pristine SPEEK membrane (43.32 mS cm^{-1}). The high surface area of 2D nanoflakes and sulfonated groups of S-TaS_2 are major factors explaining the obtained results. The M_S, M_{run5}, and M_{opt} membrane show an E_a of 18.1, 15.46, and 14.89 kJ mol^{-1}, respectively. Noteworthy, the E_a decreases with increasing the wt% of S-TaS_2 nanoflakes. A dense population of the S-TaS_2 nanoflakes in the structure of membrane can build up effective transfer pathways by reducing the distance between proton jump sites, leading to a lowering of the E_a.

S5. Mechanical stability analysis

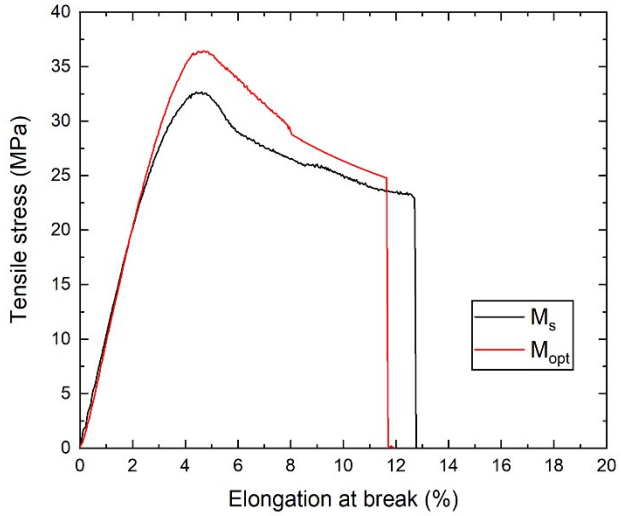

Fig. S4 Stress-strain curves measured for M_S and M_{opt}.

S6. TGA analysis

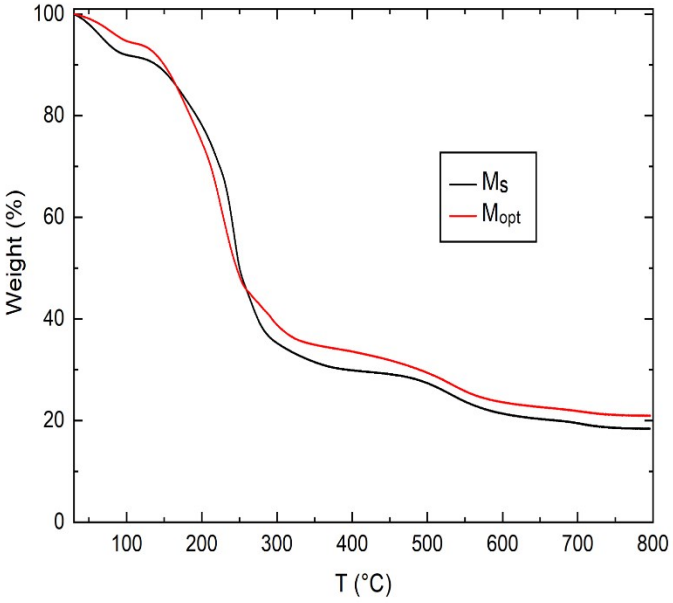

Fig. S5 TGA curves of the M_S and M_{opt}.

S.7 RSM analysis

RSM optimization is applied to show the impact of the DS and S-TaS_2 content in terms of WU value. The mathematical relationship obtained with the statistical software (Design of expert (DOE)) was a polynomial equation representing the quantitative effect of process variables and their interactions on the measured response. The second-order polynomial equation of the response surface used to predict the WU of the membranes included various amount of S-TaS_2 nanoflakes and DS are:

$$WU\ 20 = +40.58 + 3.72A + 1.38B + 0.5275AB - 0.1653A^2 - 0.8353B^2 + 1.84A^2B - 0.3775AB^2 + 0.0000A^3 + 0.0000B^3$$

$$WU\ 40 = +44.53 + 3.35A + 1.25B + 0.4750AB - 0.1542A^2 - 0.7567B^2 + 1.66A^2B - 0.3425AB^2 + 0.0000A^3 + 0.0000B^3$$

$$WU\ 60 = +49.16 + 3.01A + 1.12B + 0.4300AB - 0.1341A^2 - 0.6766B^2 + 1.49A^2B - 0.3075AB^2 + 0.0000A^3 + 0.0000B^3$$

$$WU\ 80 = +61.73 + 5.34A + 1.29B + 1.51AB + 0.7350A^2 - 0.8283B^2 + 2.74A^2B - 1.21AB^2 + 0.0000A^3 + 0.0000B^3$$

in which, A and B are the coded values for the DS of the SPEEK and wt% of S-TaS_2 nanoflakes, respectively. The equations are a linear and quadratic relationship between WU value and A and B at different temperatures. ANOVA analysis of the impact of the noise on the WU at 20 °C is tabulated in Table S2. The Model F-value of 219.98 indicates that the model is significant. There is only a 0.01% chance that an F-value this large could occur due to noise. P-values less than 0.0500 indicate that the model terms are significant. In this case A, B, AB, B^2, A^2B are significant model terms. Values greater than 0.1000 indicate that the model terms are not significant. The Lack of Fit F-value of 0.0020 implies that the Lack of Fit is not significant relative to the pure

error. There is a 96.68% chance that a Lack of Fit F-value this large could occur due to noise. Non-significant Lack of Fit is fine parameter.

Table S2 ANOVA analysis of the impact of the noise on the WU

Source	Sum of Squares	df	Mean Square	F-value	p-value	
Model	229.64	7	32.81	219.98	< 0.0001	significant
A-DS	110.71	1	110.71	742.36	< 0.0001	
B-S-TaS_2	15.35	1	15.35	102.90	0.0002	
AB	1.11	1	1.11	7.46	0.0412	
A^2	0.6261	1	0.6261	4.20	0.0958	
B^2	15.99	1	15.99	107.21	0.0001	
A^2B	9.05	1	9.05	60.70	0.0006	
AB^2	0.3800	1	0.3800	2.55	0.1713	
A^3	0.0000	0				
B^3	0.0000	0				
Residual	0.7456	5	0.1491			
Lack of Fit	0.0004	1	0.0004	0.0020	0.9668	not significant
Pure Error	0.7453	4	0.1863			
Cor Total	230.38	12				

The polynomial equation of the response surface for the MS obtained by DOE software (Table S2) are:

MS 20 = -26.17654 + 0.546222 A - 1.45667 B

MS 40 = -35.04423 + 0.710222 A - 1.89000 B

MS 60 = -33.06423 + 0.710222 A - 1.89000 B

MS 80 = -44.33538 + 0.928444 A - 2.48000 B

The Model F-value of 64.44 implies that the model is significant. There is only a 0.01% chance that an F-value this large could occur due to noise. P-values lower than 0.0001 imply that the model terms are significant. As mentioned, P-values higher than 0.1000 show that the model terms are not significant. The Lack of fit F-value of 3.79 implies that the Lack of fit is not significant relative to the pure error that is fine. There is a 10.91% chance that a Lack of Fit F-value this large could occur due to noise.

Table S3 ANOVA analysis of the impact of the noise on the MS

Source	Sum of Squares	df	Mean Square	F-value	p-value	
Model	56.71	2	28.36	64.44	< 0.0001	significant
A-DS	50.35	1	50.35	114.41	< 0.0001	
B-S-TaS_2	6.37	1	6.37	14.47	0.0035	
Residual	4.40	10	0.4401			
Lack of Fit	3.74	6	0.6237	3.79	0.1091	not significant
Pure Error	0.6588	4	0.1647			
Cor Total	61.11	12				

RSM optimization is applied to show the impact of the investigated parameters in terms of σ. The second-order polynomial equations of the response surface for the obtained σ are:

$$\sigma\ 20 = + 82.25 + 13.86A + 2.87\ B + 0.0000\ AB + 1.50\ A^2 - 2.84\ B^2 + 5.45\ A^2B - 6.93\ AB^2$$

$$\sigma\ 40 = + 93.32 + 17.33\ A + 3.58\ B + 0.0000\ AB + 1.88\ A^2 - 3.55\ B^2 + 6.81\ A^2B - 8.66\ AB^2$$

$$\sigma\ 60 = + 111.65 + 19.40\ A + 4.01\ B + 0.0000\ AB + 2.10\ A^2 - 3.98\ B^2 + 7.63\ A^2B - 9.70\ AB^2$$

$$\sigma\ 80 = + 142.93 + 23.56\ A + 4.87\ B + 0.0000\ AB + 2.55\ A^2 - 4.83\ B^2 + 9.26\ A^2B - 11.78\ AB^2$$

The equation in terms of coded factors can be used to make predictions about the response for given levels of each factor. The coded equation is useful for identifying the relative impact of the factors by comparing the factor coefficients. The above equations are a linear and quadratic relationship between parameters and σ at different temperatures. ANOVA analysis of the impact of the noise on the σ at 20 °C is tabulated in Table S4. The Model F-value of 72.90 implies that the model is significant. There is only a 0.01% chance that an F-value this large could occur due to noise. P-values less than 0.0500 indicate that the model terms are significant. In this case A, B, A^2, B^2, A^2B, AB^2 are significant model terms. Values greater than 0.1000 indicate that the model terms are not significant. If there are many insignificant model terms (not counting those required to support hierarchy), model reduction may improve the model. The Lack of Fit F-value of 1.17 implies that the Lack of Fit is not significant relative to the pure error. There is a 33.97% chance that a Lack of Fit F-value this large could occur due to noise. Non-significant lack of Fit is fine.

Table S4 ANOVA analysis of the impact of the noise on the σ

Source	Sum of Squares	df	Mean Square	F-value	p-value	
Model	2388.90	7	341.27	72.90	< 0.0001	significant
A-DS	1536.80	1	1536.80	328.27	< 0.0001	
B-S-TaS_2	65.73	1	65.73	14.04	0.0133	
AB	0.0000	1	0.0000	0.0000	1.0000	
A^2	51.60	1	51.60	11.02	0.0210	
B^2	184.95	1	184.95	39.51	0.0015	
A^2B	79.19	1	79.19	16.92	0.0092	
AB^2	128.07	1	128.07	27.36	0.0034	
A^3	0.0000	0				
B^3	0.0000	0				
Residual	23.41	5	4.68			
Lack of Fit	5.31	1	5.31	1.17	0.3397	not significant
Pure Error	18.10	4	4.53			
Cor Total	2412.31	12				

The second-order polynomial equations of the response surface obtained which can be used to predict the P of membranes included various amount of the S-TaS_2 nanoflakes and DS are:

$$P\ 20 = + 2.03 + 0.1860\ A + 0.0692\ B + 0.0264\ AB - 0.0083\ A^2 - 0.0418\ B^2 + 0.0921\ A^2B - 0.0189\ AB^2$$

The Model F-value of 219.98 shows that the model is significant. There is only a 0.01% chance that an F-value this large could occur due to noise. Also, the P-values less than 0.0500 indicate that the model terms are significant. In this case A, B, AB, B^2, A^2B are significant model terms. Values greater than 0.1000 indicate that the model terms are not significant. The Lack of Fit F-value of 0.00 implies that the Lack of Fit is not significant relative to the pure error that it is fine. There is a 96.68% chance that a Lack of Fit F-value this large could occur due to noise.

Table S5 ANOVA analysis of the impact of the noise on the P

Source	Sum of Squares	df	Mean Square	F-value	p-value	
Model	0.5741	7	0.0820	219.98	< 0.0001	significant
A-DS	0.2768	1	0.2768	742.36	< 0.0001	
B-S-TaS_2	0.0384	1	0.0384	102.90	0.0002	
AB	0.0028	1	0.0028	7.46	0.0412	
A^2	0.0016	1	0.0016	4.20	0.0958	
B^2	0.0400	1	0.0400	107.21	0.0001	
A^2B	0.0226	1	0.0226	60.70	0.0006	
AB^2	0.0010	1	0.0010	2.55	0.1713	
A^3	0.0000	0	0.0820	219.98	< 0.0001	
B^3	0.0000	0				
Residual	0.0019	5	0.0004			
Lack of Fit	9.121E-07	1	9.121E-07	0.0020	0.9668	not significant
Pure Error	0.0019	4	0.0005			
Cor Total	0.5760	12				

The second-order polynomial equations for prediction of S of membranes included various amount of the S-TaS_2 nanoflakes and DS is:

$$S\ 20 = +\ 34.53 + 1.15\ A + 8.28\ B + 1.70\ AB - 3.89\ A^2 - 1.33\ B^2$$

The Model F-value of 11.50 implies that the model is significant. There is only a 0.29% chance that an F-value this large could occur due to noise. P-values less than 0.0500 indicate that the model terms are significant. In this case B, A^2 are significant model terms. Values greater than 0.1000 indicate that the model terms are not significant. The Lack of Fit F-value of 1.51 implies that the Lack of Fit is not significant relative to the pure error. There is a 34.06% chance that a Lack of Fit F-value this large could occur due to noise. Non-significant Lack of Fit is fine.

Table S6 ANOVA analysis of the impact of the noise on the S

Source	Sum of Squares	df	Mean Square	F-value	p-value	
Model	1199.06	5	239.81	11.50	0.0029	significant
A-DS	15.87	1	15.87	0.7613	0.4118	
B-S-TaS_2	823.36	1	823.36	39.50	0.0004	
AB	11.56	1	11.56	0.5546	0.4807	
A^2	347.01	1	347.01	16.65	0.0047	
B^2	40.48	1	40.48	1.94	0.2061	
Residual	145.92	7	20.85			
Lack of Fit	77.51	3	25.84	1.51	0.3406	not significant
Pure Error	68.41	4	17.10			
Cor Total	1344.98	12				

S.7 Comparison of membranes

Table S7 Comparison between WU, σ, P, and power density of the M_{opt} membrane with Nafion and SPEEK membranes used in DMFC at room temperature.

Membranes	σ (S/cm)	P ($cm^2\ s^{-1}$)	S ($S\ s^{-1}\ cm^{-3}$)	Power density ($mW\ cm^{-2}$)	Ref
M_{opt}	0.096	2.66×10^{-7}	36.18×10^{4}	64.55	This Work
SPEEK/CN[a]	0.079	5.03×10^{-7}	3.75×10^{4}	-	[15]
SPEEK/BPPO[b]	0.029	3.69×10^{-7}	7.94×10^{4}	56.00	[16]
SPEEK/SHGO[c]	0.090	3.83×10^{-6}	2.34×10^{4}	29.00	[17]
Semi-IPN[d] SPEEK	0.059	3.26×10^{-7}	18.12×10^{4}	32.50	[18]
SPEEK/HPW/g-C_3N_4[e]	0.051	3.04×10^{-7}	17.10×10^{4}	13.00	[19]
TA[f]-SPEEK	0.085	2.19×10^{-7}	38.80×10^{4}	35.30	[20]
Nafion/aminated SPEEK	0.064	8.92×10^{-7}	7.17×10^{4}	26.00	[21]
Nafion 117	0.090	2.40×10^{-6}	3.75×10^{4}	24.00	[22]
Nafion 115	0.086	1.83×10^{-6}	4.75×10^{4}	31.80	[20]

[a]; Graphitic carbon nitride nanosheets [b]; Bromomethylated poly(phenylene oxide) [c]; Sulfonated holey graphene oxide [d]; Semi-interpenetrating polymer networks [e]; Phosphotungstic acid/carbon nitride [f]; Tertiary amine

Refrences

1 H. Beydaghi, M. Javanbakht, A. Bagheri, P. Salarizadeh, H. G. Zahmatkesh, S. Kashefi and E. Kowsari, *RSC Adv.*, , DOI:10.1039/c5ra12941a.

2 L. Najafi, S. Bellani, R. Oropesa-Nuñez, B. Martín-García, M. Prato, L. Pasquale, J.-K. Panda, P. Marvan, Z. Sofer and F. Bonaccorso, *ACS Catal.*, 2020, **10**, 3313–3325.

3 L. Najafi, S. Bellani, R. Oropesa-Nuñez, B. Martín-García, M. Prato, V. Mazánek, D. Debellis, S. Lauciello, R. Brescia, Z. Sofer and F. Bonaccorso, *J. Mater. Chem. A*, 2019, **7**, 25593–25608.

4 F. Bonaccorso, A. Bartolotta, J. N. Coleman and C. Backes, *Adv. Mater.*, 2016, **28**, 6136–6166.

5 V. Nicolosi, M. Chhowalla, M. G. Kanatzidis, M. S. Strano and J. N. Coleman, *Science (80-.).*, 2013, **340**, 1226419.

6 H. Beydaghi, A. Bagheri, P. Salarizadeh, S. Kashefi, K. Hooshyari, A. Amoozadeh, T. Shamsi, F. Bonaccorso and V. Pellegrini, *Ind. Eng. Chem. Res.*, , DOI:10.1021/acs.iecr.9b06813.

7 C. Li, Z. Yang, X. Liu, Y. Zhang, J. Dong, Q. Zhang and H. Cheng, *Int. J. Hydrogen Energy*, 2017, **42**, 28567–28577.

8 H. Ilbeygi, A. Mayahi, A. F. Ismail, M. M. Nasef, J. Jaafar, M. Ghasemi, T. Matsuura and S. M. J. Zaidi, *J. Taiwan Inst. Chem. Eng.*, 2014, **45**, 2265–2279.

9 M. H. Dehghani, Z. S. Niasar, M. R. Mehrnia, M. Shayeghi, M. A. Al-Ghouti, B. Heibati, G. McKay and K. Yetilmezsoy, *Chem. Eng. J.*, 2017, **310**, 22–32.

10 A. Bagheri, P. Salarizadeh, M. Sabooni Asre Hazer, P. Hosseinabadi, S. Kashefi and H. Beydaghi, *Electrochim. Acta*, , DOI:10.1016/j.electacta.2018.10.197.

11 https://www.itl.nist.gov/div898/handbook/pri/section3/pri3361.htm, https://www.itl.nist.gov/div898/handbook/pri/section3/pri3361.htm.

12 A. Mayahi, A. F. Ismail, H. Ilbeygi, M. H. D. Othman, M. Ghasemi, M. N. A. M. Norddin and T. Matsuura, *Sep. Purif. Technol.*, 2013, **106**, 72–81.

13 H. Maab, M. Schieda, W. Yave, S. Shishatskiy and S. P. Nunes, *Fuel Cells*, 2009, **9**, 401–409.

14 T. Y. Inan, H. Doğan, E. E. Unveren and E. Eker, *Int. J. Hydrogen Energy*, 2010, **35**, 12038–12053.

15 M. Gang, G. He, Z. Li, K. Cao, Z. Li, Y. Yin, H. Wu and Z. Jiang, *J. Memb. Sci.*, 2016, **507**, 1–11.

16 X. Liu, Y. Zhang, S. Deng, C. Li, J. Dong, J. Wang, Z. Yang, D. Wang and H. Cheng, *ACS Appl. Energy Mater.*, 2018, **1**, 5463–5473.

17 Z.-J. Jiang, Z. Jiang, X. Tian, L. Luo and M. Liu, *ACS Appl. Mater. Interfaces*, 2017, **9**, 20046–20056.

18 X. Liu, Y. Zhang, S. Deng, C. Li, J. Dong, J. Wang, Z. Yang, D. Wang and H. Cheng, *Chinese Chem. Lett.*, 2019, **30**, 299–304.

19 C. Dong, Q. Wang, C. Cong, X. Meng and Q. Zhou, *Int. J. Hydrogen Energy*, 2017, **42**, 10317–10328.

20 L. Lei, X. Zhu, J. Xu, H. Qian, Z. Zou and H. Yang, *J. Power Sources*, 2017, **350**, 41–48.

21 J.-C. Tsai and C.-K. Lin, *J. Taiwan Inst. Chem. Eng.*, 2011, **42**, 281–285.

22 Q. He, J. Zheng and S. Zhang, *J. Power Sources*, 2014, **260**, 317–325.